Dry deposition of reactive nitrogen to European ecosystems: a comparison of inferential models across the NitroEurope network – Supplementary Material

C. R. Flechard, E. Nemitz, R. I. Smith, D. Fowler, A. T. Vermeulen, A. Bleeker, J.W. Erisman, D. Simpson, L. Zhang, Y. S. Tang and M. A. Sutton

A1 Introduction

This supplement provides additional details concerning the implementation of four dry deposition (inferential) routines as part of the model inter-comparison at the ecosystem scale presented in the aforementioned article, with respect to ecosystem characteristics, micrometeorology and canopy wetness simulation.

A2 Canopy characteristics

For the modelling of trace gas and particle deposition at national or regional scales, the inferential routines of the four models (i.e. CBED, CDRY, EMEP-03, IDEM) normally use either land use class (LUC)-specific, monthly default values, or phenological functions, for the key canopy characteristics (canopy height h_c, roughness length z_0 and leaf area index LAI), since such data are not available at the ecosystem scale for every node of the grid domain nor for every day of the year. These default values or functions for each LUC logically differ between the four models since they were developed for different countries or climatic zones.

In this paper, however, the models are applied locally to a number of ecosystem study sites, rather than to a whole geographical domain. Measurements of h_c and of LAI were made as part of CarboEurope IP at most sites of the NitroEurope (NEU) inferential network (Table 1 of main paper). These measurements were carried out typically a few times during the growing season but the data capture was very uneven between sites. While the temporal (seasonal) variations were extremely well documented with very frequent (weekly) measurements at a few sites of the network, too few data were available at the majority of the other sites to reliably interpolate over time, as required for input to deposition models. This is largely due to the fact that in many cases only the maximum LAI was recorded during the growing season, while the conditions at the start and end of the growing season can only be guessed. With several cuts per year in grasslands, or more than one crop per year in arable systems, the frequent measurements needed were not available for all sites. There was also the added problem that the NEU project (2006-2010) was shifted in time relative to CarboEurope IP (2004-2008), so that much of the LAI and h_c data collected as part of CarboEurope were not contemporaneous with the NEU trace gas and aerosol datasets (initiated in 2007). Another difficulty resides in the method or type of LAI measurement (single-sided, double-sided, projected, total) not being recorded, so that the available data may not be compatible with the input required for modelling.

Based on these considerations, model base runs in this study use model default values of LAI, combined with time-interpolated values of h_c derived from the available measured data (‘ModLAI / MeasHc’, see Table A2). The choice of model default LAI is primarily motivated by the potentially large error in measured LAI data, which may be considered just as uncertain as model default values. By contrast, h_c is a more easily measured and defined canopy characteristic, which can arguably be considered constant for forests over the time frame of CarboEurope and NEU. More importantly, the measurement heights for the sonic anemometers and for the DELTA gas and aerosol sampling apparatus were in practice set according to the true h_c. Thus the measured pollutant concentrations reflected vertical gradients and turbulent mixing conditions consistent with the real h_c, but not necessarily with a model default value.

Nevertheless, if the objective is to fully inter-compare models, rather than obtain the ‘truest’ model deposition estimates, one could argue that h_c and LAI descriptions in default lookup tables can be regarded as intrinsic model parameters, and should therefore both be used as inputs (‘ModLAI / ModHc’). Conversely, using both sets of measured LAI and h_c as common inputs to the four models (‘MeasLAI / MeasHc’) could be defended as providing a better set-up for inter-comparing the models treatment of surface resistances, in which the confounding effects of surface roughness and area are removed. These alternative choices for the model inputs values of LAI and h_c are presented to assess the sensitivity of annual dry deposition fluxes (Figure A2). For the reconstruction of seasonal time series of daily h_c and LAI, the data were interpolated between consecutive measurements if their time resolution was sufficient;

alternatively, generic annual curves were computed on the basis of the standard EMEP-03 phenological functions (Simpson et al., 2003), then scaled using the measured minimum and maximum values at each site.

A3 Micrometeorological data

Fundamental variables needed to compute the atmospheric resistances R_a and R_b include u_*, sensible heat flux H, and z_0. At 51 of the 55 sites of the NEU inferential network, long-term eddy covariance (EC) measurements of CO_2 and H_2O exchange were carried out within the framework of CarboEurope IP (Aubinet et al., 2000), and thus actual in-situ measurements of u_* and H were available on a half-hourly basis and obtained courtesy of the CarboEurope-IP database. For the 4 remaining non-CarboEurope IP sites (DE-Hoe, FI-Lom, NL-Spe, UA-Pet), eddy covariance flux measurements were initiated as part of NitroEurope IP. In the base model runs presented hereafter, all available measured (EC) u_* and H data were used by default for the calculation of atmospheric resistances.

For cases when valid turbulence data from EC were not available due to instrument failure, strong nocturnal atmospheric stability, small wind speeds or insufficient fetch (Aubinet et al., 2000), u_* and H needed to be gap-filled from standard meteorological data (wind speed, net radiation, temperature) measured at each site. This was done in a similar fashion to meteorological sub-modules of regional chemical transport models (CTMs), which derive their u_* from numerical weather prediction (NWP) model output data, such that (Thom, 1975):

$$u_* = \frac{\kappa U\left(z_{ref} - d\right)}{\left[\ln\left(\frac{z_{ref} - d}{z_0}\right) - \psi_{\mathrm{M}}\left(\frac{z_{ref} - d}{L}\right) + \psi_{\mathrm{M}}\left(\frac{z_0}{L}\right)\right]} \qquad \text{(A1)}$$

where z_0 is roughness length and d is displacement height, both being dependent on h_c, U is wind speed, κ is von Karman's constant (= 0.41), ψ_M is the integrated atmospheric stability correction function for momentum, and L is the Obukhov stability length:

$$L = -\frac{\rho_a \theta C_p u_*^{\,3}}{\kappa g H} \qquad \text{(A2)}$$

with ρ_a the density of dry air (g m^{-3}), θ the potential air temperature (K), C_p the specific heat capacity of air (= 1.005 J g^{-1} K^{-1}) and g the gravitational acceleration (= 9.81 m s^{-2}) (Thom, 1975). However, this also requires the knowledge of L, which is itself a function of both u_* and H (Eq. A2). In the absence of valid micrometeorological measurements, a first and necessary step adopted here as in other models (e.g. Bassin et al., 2004) consists in a rough estimation of H assuming the closure of the surface energy balance and a partitioning of the available energy such that:

$$H = R_n - \lambda E - G \qquad \text{(A3)}$$

Here G is the ground heat flux, and the latent heat flux λE was estimated using the Penman-Monteith (P-M) equation, which may only be done in a first approximation assuming neutral stratification, since H and L are both unknown. As R_a and R_s are also needed, as rather poorly quantified drivers of evaporation, in the P-M equation, both estimates of λE and H are necessarily quite uncertain, all the more as the surface energy closure assumption is often not confirmed in the field (e.g. Wohlfahrt et al., 2009). From the H estimate thus obtained, both u_* and L are then calculated iteratively using Eqs. (A1) and (A2). The overall effect of the gap-filling procedure for H on annual N_r fluxes appears to be small, however, as the error in H does not propagate very strongly into u_* (Bassin et al., 2004), and also because micrometeorological data gaps are by nature strongly correlated with periods of reduced wind speeds and suppressed turbulence, during which potential rates of tracer exchange are very small.

A4 Surface potentials

For the calculation of stomatal and non-stomatal resistances, and of the NH_3 compensation point (Eqs. 3 to 10 in main Paper), values of the surface scalars temperature and relative humidity are required. From the viewpoint of a numerical weather prediction (NWP) model, ‘surface’ actually means anything between the measurement height (z_{ref}) of a standard meteorological station within the surface layer, typically 2-3 m above ground or up to 10 meters above tree tops in the case of a forest, up to 50-100 m. From a micrometeorological, field-scale point of view, ‘surface’ corresponds to the notional height $z_s = d+z_0$’, ‘below’ the viscous sublayer, with z_0’ the roughness length for heat and trace gases (Monteith and Unsworth, 1990). There can be substantial differences between scalars at z_s and z_{ref}, depending on the intensity of turbulent mixing, canopy roughness, solar radiation and atmospheric thermal stratification, especially over short vegetation. The temperature difference between z_s and z_{ref} has a particularly strong impact on the calculation of the stomatal compensation point (χ_s), which increases exponentially with temperature and doubles approximately with every additional 4 – 5 K (Flechard and Fowler, 2008; Personne et al., 2009), while for stomatal resistance the *vpd* stress factor f_e is best evaluated using relative humidity at z_s.

By default in this paper, model base runs used ambient temperature and relative humidity data as measured by meteorological stations at z_{ref}, a few m above vegetation, which is the closest approximation to the outputs of NWP models that are normally used as inputs to CTMs. The sensitivity of modelled fluxes to input *T* and *RH* was however tested in alternative model runs by using the potentials at z_s rather than z_{ref} as input to the deposition routines (see 'Surface potentials' model runs in Table A2 and Fig. A2). The z_s potentials were first computed from measured micrometeorological fluxes of both sensible (*H*) and latent heat (λE), following (e.g. Monteith and Unsworth, 1990):

$$T(z_0') = T(z_{ref} - d) + \frac{H}{\rho C_p}\left(R_a(z_{ref} - d) + R_{b,heat}\right) \quad \text{(A4)}$$

and

$$e(z_0') = e(z_{ref} - d) + \frac{pE}{\rho \varepsilon}\left(R_a(z_{ref} - d) + R_{b,H_2O}\right) \quad \text{(A5)}$$

where *e* is water vapour pressure, *p* is atmospheric pressure, *E* is the water vapour flux and ε is the ratio of the molecular weight of water to the mean molecular weight of dry air (= 18/29), and the surface relative humidity is given by

$$RH(z_0') = \frac{e(z_0')}{e_{sat}(T(z_0'))} \quad \text{(A6)}$$

where $e_{sat}(T)$ is the saturation water vapour pressure at *T*.

A5 Canopy wetness

Surface wetness controls non-stomatal resistances for soluble trace gases in all four models, particle rebound (EMEP-03, CDRY), and even stomatal 'blocking' (CDRY). Depending on the process, chemical species and model considered, the wetness effect is either quantified by a continuous function of *RH* (e.g. Eq. 4-7 in main paper), or qualified by a binary (or boolean) indicator (wet =1 or true, dry =0 or false), with different surface resistances for the dry and wet cases. In the IDEM model, both a wetness indicator and the *RH* function (Eq. (7) in main paper) are used in turns for R_{ext} in the case of NH_3. Canopy wetness was actually monitored at a few sites of the NEU network (e.g. BE-Bra, CH-Oe1, NL-Spe, FR-Gri, UK-Amo) using surrogate sensors (e.g. Model 237 Leaf Wetness Sensor, Campbell Scientific, Logan, UT), but at most sites no measurements were available. For models in which a wetness boolean was required, this needed to be estimated from ancillary environmental data.

Although modelled R_w, R_c and deposition flux are highly sensitive to wetness, canopy wetness is difficult to predict reliably. This is compounded by the fact that, although a leaf surface may appear dry to the eye or to surrogate wetness sensors, thin water films on microscopic scales, as demonstrated by leaf wetness/conductivity clips (Burkhardt and Eiden, 1994), still provide sinks for atmospheric gases, and thus a leaf surface might seldom be fully 'dry'. Various *RH* thresholds have been used as proxies to determine canopy wetness; van Jaarsveld (2004) determines a dry-wet switch point of 87% from surface wetness observations over mixed forest, while for grassland Wichink Kruit et al. (2008, 2010) suggest a smaller threshold at 71%. Both studies used ambient (z_{ref}) *RH* data, but it could be that the same analyses using $RH(d+z_0')$ (see Section A4) might have yielded thresholds which were more similar to each other, given the larger vertical *RH* gradients over grassland than over forest. Some dry deposition models such as CDRY predict surface wetness semi-mechanistically and distinguish dew from rain, based on precipitation data and on night-time cloud cover and u_* for dew formation. Other models either treat wetness as an input variable provided e.g. by NWP models, or use rule-of-thumb decisions based on ambient *RH* and precipitation. The CBED model does not actually require any wetness indicator to quantify the non-stomatal resistance for N_r gases.

Since the treatment of surface wetness prediction by the inferential models is rather crude and model-dependent, and since surface wetness can be regarded as an input variable to the models (rather than an output), it was preferred here to use a common wetness parameterisation to feed all four models. This suppresses the inter-model variability that would caused by differing wetness schemes, and allows the model intercomparison to focus on discrepancies in surface resistances and fluxes. The approach used to simulate common wetness data was based on the mechanistic, big leaf, surface wetness energy balance (SWEB) and canopy water budget model by Magarey et al. (2006). The SWEB model was originally designed for grapes but model canopy characteristics (LAI, h_c) can be adjusted to deal with other crops and vegetation types. Inputs to the model are T and RH at the canopy height, precipitation, wind speed U measured at z_{ref}-d above the canopy and R_n. The model is dynamic, allowing surface water to accumulate up to the maximum storage capacity and to evaporate depending on meteorological conditions. The model therefore requires continuous input data, which were routinely available from meteorological stations at each site of the network. For cases when key meteorological variables were missing to run SWEB, but ambient RH was still available, canopy wetness was decided on the basis of a wet-dry threshold of 81%, which corresponds to the deliquescence point of ammonium sulphate (Flechard et al., 1999), although in reality deposited material on leaf surfaces is a mixture of various salts and organic aerosols. For the CDRY model, which requires a distinction of dew- from rain-wetted surfaces, the output of SWEB was split following CDRY decision rules.

The SWEB scheme (Magarey et al., 2006) was run systematically, regardless of the inferential model used, but the wetness output was slightly model-dependent, due to the differences in model LAI defaults. SWEB outputs are evaluated and compared in Fig. A1 with measured data at five sites of the network, which were equipped with surrogate leaf wetness sensors (BE-Bra, CH-Oe1, FR-Gri, NL-Spe and UK-Amo). The data show the frequency (or probability) of wetness occurrence as a function of the time of day; there are strong seasonal variations that are driven by meteorological conditions, but for clarity the data are here averaged over the whole year. All sites describe a strong diurnal cycle, with the largest wetness frequency occurring toward late night/early morning, and the driest period occurring in mid to late afternoon, consistent with night-time dewfall and daytime evaporation of foliar wetness. The occurrence of rainfall may be considered to be randomly distributed through the day, having thus no effect on the shape of the diurnal cycle, though this is probably not be true for all sites.

Diurnal patterns and overall average wetness frequency are broadly consistent between observations and modelled values. The “wettest” canopy was found at the cut grassland site CH-Oe1 in both measurements and model simulations, with a night-time frequency of 90% and a daytime minimum of 40%. By contrast the other sites showed a night-time wetness probability of 50-80% and daytime minima of typically 20-30%. This was consistent with the average annual rainfall being largest at CH-Oe1 (1200 mm). CH-Oe1 and FR-Gri had frequent dewfall due to frequent night-time inversions in semi-continental climates, while BE-Bra, NL-Spe and UK-AMo are windier sites in more oceanic conditions.

Differences between the various SWEB model runs at each site shown in Fig. A1 can essentially be ascribed to the canopy-scale, leaf surface wetness storage capacity, and consequently the different average leaf wetness durations, which are driven by different LAI defaults from each model. For example at the arable site of FR-Gri, the model run using EMEP-03 LAI defaults provided much smaller wetness frequencies than the other models, which was consistent with a much smaller mean annual LAI in EMEP-03 (0.42) than in CBED (1.35), CDRY (1.22) and IDEM (1.72). SWEB was also run for comparison using estimates of LAI provided at each site. At BE-Bra, CH-Oe1 and FR-Gri this did not significantly improve nor lessen SWEB performance, as compared with observations, but at NL-Spe and UK-AMo there was a noticeable improvement for night-time conditions, where observations apparently indicated much less frequent wetness occurrences than the canopy water budget approach.

It should be noted that “observed” wetness measurements can have significant uncertainties, and for example the small wetness values seen at night-time at the blanket bog site UK-AMo seem somewhat surprising (one would expect almost 100% humidity near the surface at night at such sites, which ought to cause wetness), but the representativity of, and the potential errors in, wetness measurements made using generally only one surrogate sensor cannot be assessed here and have been treated elsewhere (e.g. Wichink Kruit et al., 2008). The lack of spatial or vertical resolution in such data and the different behaviours of wetness sensors and leaves or needles with respect to water evaporation, condensation and to particle deposition, which favours condensation at smaller *RH* (Burkhardt and Eiden, 1994), might explain some of the discrepancies oberved between measurements and models. On the other hand, any surface wetness and energy balance approach will suffer shortcomings and may perform better for certain types of vegetation than others. It is perhaps not surprising that the SWEB model by Magarey et al. (2006), having been developed for agricultural vegetation, seemed to give best results over grass at CH-Oe1 and cropland at FR-Gri, but in forests (BE-Bra, NL-Spe in Fig. A1) big leaf limitations may be significant. More validation data are required, but based on the few sites where a comparison was performed (Fig. A1), the SWEB approach may be considered robust and valid for the purposes of inferential modelling.

A6 References

Aubinet, M., Grelle, A., Ibrom, A., Rannik, U., Moncrieff, J., Foken, T., Kowalski, A.S., Martin, P.H., Berbigier, P., Bernhofer, Ch., Clement, R., Elbers, J., Granier, A., Grünwald, T., Morgenstern, K., Pilegaard, K., Rebmann, C., Snijders,W., Valentini, R. and Vesala, T.: Estimates of the annual net carbon and water exchange of forests: the EUROFLUX methodology, Adv. Ecol. Res., 30, 113–171, 2000.

Bassin, S., Calanca, P., Weidinger, T., Gerosa, G. and Fuhrer, J.: Modelling seasonal ozone fluxes to grassland and wheat: model improvement, testing, and application, Atmos. Environ., 38, 2349-2359, 2004.

Burkhardt, J. and Eiden, R.: Thin water films on coniferous needles, Atmos. Environ., 28, 2001-2011, 1994.

Flechard, C.R., Fowler, D., Sutton, M.A., and Cape, J.N.: A dynamic chemical model of bi-directional ammonia exchange between semi-natural vegetation and the atmosphere, Q. J. Roy. Meteor. Soc., 125, 2611-2641, 1999.

Flechard, C.R. and Fowler, D.: Effects of Changing Temperature on Leaf Surface Water-Film Chemistry and Trace Gas Exchange Processes over Terrestrial Vegetation, in: The Impact of Climate Change on Air Quality, The 4th ACCENT Barnsdale Expert Workshop, Editors: P. Builtjes, D. Fowler, J. Feichter, A. Lewis, P. Monks and P. Borrell, ACCENT Secretariat, Urbino, 155–161, 2008.

Magarey, R.D., Russo, J.M. and Seem, R.C.: Simulation of surface wetness with a water budget and energy balance approach, Agr. Forest Meteorol., 139, 373–381, 2006.

Monteith, J.L. and Unsworth, M.H.: Principles of Environmental Physics, 2nd edition. Edward Arnold, London. 291 pp, 1990.

Personne, E., Loubet, B., Herrmann, B., Mattsson, M., Schjoerring, J.K., Nemitz, E., Sutton, M.A. and Cellier, P.: SURFATM-NH3 : a model combining the surface energy balance and bi-directional exchanges of ammonia applied at the field scale, Biogeosciences, 6, 1371–1388, 2009.

Simpson, D., Fagerli, H., Jonson, J.E., Tsyro, S., Wind, P. and Tuovinen, J.-P.: Transboundary Acidification, Eutrophication and Ground Level Ozone in Europe. Part I:

Unified EMEP Model Description, EMEP Status Report 2003, ISSN 0806-4520, Det Meteorologisk Institutt, Oslo, 2003.

Thom, A.S.: Momentum, mass and heat exchange of plant communities. In: Vegetation and the atmosphere, vol. 1 (Ed: J.L. Monteith), pp 57-109. Academic Press, London, 1975.

van Jaarsveld J.A.: The Operational Priority Substances model: Description and validation of OPS-Pro 4.1, RIVM report 500045001/2004, 156 pp., Bilthoven, The Netherlands, 2004.

Wichink Kruit, R.J., Jacobs, A.F.G. and Holtslag, A.A.M.: Measurements and estimates of leaf wetness over agricultural grassland for dry deposition modelling of trace gases, Atmos. Environ., 42, 5304-5316, 2008.

Wichink Kruit, R.J., van Pul, W.A.J., Sauter, F.J., van den Broek, M., Nemitz, E., Sutton, M.A., Krol, M. and Holtslag, A.A.M.: Modelling the surface-atmosphere exchange of ammonia, Atmos. Environ., 44 (7), 945-957, 2010.

Wohlfahrt, G., Haslwanter, A., Hörtnagl, L., Jasoni, R.L., Fenstermaker, L.F., Arnone, J.A. and Hammerle, A.: On the consequences of the energy imbalance for calculating surface conductance to water vapour, Agr. Forest Meteor., 149, 1556-1559, 2009.

Table A1. Selected references for the measurement sites

Site Code	Site Name	Authors	Year	Journal	Vol.	Pages
BE-Bra	Brasschaat	Neirynck et al.	2005	Atmos. Environ.	39	5013-5024
BE-Vie	Vielsalm	Heinesch et al.	2007	Boundary Layer Meteorol.	122	457-478
CH-Lae	Laegeren	Ruehr et al.	2010	Biogeochemistry	98	153-170
CZ-BK1	Bily Kriz	Sedlak et al.	2010	Agric. Forest Meteorol.	150	736-744
DE-Hai	Hainich	Knohl et al.	2003	Agric. Forest Meteorol.	118	151-167
DE-Hoe	Höglwald	Kreutzer et al.	2009	Plant Biol.	11	643-649
DE-Tha	Tharandt	Grünwald and Bernhofer	2007	Tellus	59B	387-396
DE-Wet	Wetzstein	Anthoni et al.	2004	Glob. Change Biol.	10	2005-2019
DK-Sor	Soroe	Pilegaard et al.	2003	Boreal Environ. Res.	8	315-333
ES-ES1	El Saler	Sanz et al.	2002	Environm. Pollution	118	259-272
ES-LMa	Las Majadas	Casals et al.	2009	Soil Biol. Biochem.	41	1915-1922
FI-Hyy	Hyytiälä	Vesala et al.	2005	Glob. Biogeochem. Cycles	19	n° GB2001
FI-Sod	Sodankylä	Thum et al.	2008	Biogeosciences	5	1625-1639
FR-Fon	Fontainbleau	Davi et al.	2006	Agric. Forest Meteorol.	139	269-287
FR-Hes	Hesse	Granier et al.	2008	Ann. For. Sci.	64	n° 704
FR-LBr	Le Bray	Rivalland et al.	2005	Ann. Geophysicae	23	291-304
FR-Pue	Puechabon	Allard et al.	2008	Glob. Change Biol.	14	714-725
IT-Col	Collelongo	Scartazza et al.	2004	Oecologia	140	340-351
IT-Ren	Renon	Marcolla et al.	2005	Agric. Forest Meteorol.	130	193-206
IT-Ro2	Roccarespampani	Tedeschi et al.	2006	Glob. Change Biol.	12	110-121
IT-SRo	San Rossore	Chiesi et al.	2005	Agric. Forest Meteorol.	135	22-34
NL-Loo	Loobos	Dolman et al.	2002	Agric. Forest Meteorol.	111	157-170
NL-Spe	Speulderbos	Erisman et al.	1999	Water, Air, and Soil Pollution	109	237-262
PT-Esp	Espirra	Pereira et al.	2007	Biogeosciences	4	791-802
PT-Mi1	Mitra II (Evora)	Pereira et al.	2007	Biogeosciences	4	791-802
RU-Fyo	Fyodorovskoye	Ramonet et al.	2002	Tellus	54B	713-734
SE-Nor	Norunda	Grelle et al.	1999	Agric. Forest Meteorol.	98-99	563-578
SE-Sk2	Skyttorp	Lindroth et al.	2008	Tellus	60B	129-142
UK-Gri	Griffin	Clement et al.	2003	Scottish Forestry	57	5-10
DE-Meh	Mehrstedt	Don et al.	2009	Glob. Change Biol.	15	1990-2002
ES-VDA	Vall d'Alinyà	Sebastià	2007	J. App. Ecology	44	158-167
FI-Lom	Lompolojänkkä	Aurela et al.	2009	Boreal Environ. Res.	14	699-710
HU-Bug	Bugac	Nagy et al.	2007	Agric. Ecosys. Environ.	121	21-29
IT-Amp	Amplero	Gavrichkova et al.	2010	Agric. Ecosys. Environ.	136	87-96
IT-MBo	Monte Bondone	Vescovo and Gianelle	2006	Agric. Ecosys. Environ.	115	141-149
NL-Hor	Horstermeer	Hendriks et al.	2007	Biogeosciences	4	411-424
PL-wet	POLWET					
UK-AMo	Auchencorth Moss	Flechard et al.	1998	Quart. J. Roy. Meteorol. Soc.	124	733-757
CH-Oe1	Oensingen	Flechard et al.	2005	Glob. Change Biol.	11	2114-2127
DE-Gri	Grillenburg	Tittebrand et al.	2009	Theor. Appl. Climatol.	98	171-186
DK-Lva	Rimi	Gryning et al.	2009	Boreal Environ. Res.	14	204-212
FR-Lq2	Laqueuille	Allard et al.	2007	Agric. Ecosys. Environ.	121	47-58
IE-Ca2	Carlow	Abdalla et al.	2009	Geoderma	151	327-337
IE-Dri	Dripsey	Byrne et al.	2005	Agric. Forest Meteorol.	135	82-92
NL-Ca1	Cabauw	Jacobs et al.	2007	Biogeosciences	4	803-816
UK-EBu	Easter Bush	Milford et al.	2001	Water Air Soil Pollution Focus	1	167-176
BE-Lon	Lonzee	Moureaux et al.	2006	Agric. Forest Meteorol.	139	25-39
DE-Geb	Gebesee	Anthoni et al.	2004	Agric. Forest Meteorol.	121	55-67
DE-Kli	Klingenberg	Tittebrand et al.	2009	Theor. Appl. Climatol.	98	171-186
DK-Ris	Risbyholm	Houborg and Soegaard	2004	Remote Sensing Environ.	93	150-167
FR-Gri	Grignon	Lamaud et al.	2009	Agric. Forest Meteorol.	149	1385-1396
IT-BCi	Borgo Cioffi	Vitale et al.	2009	Acta Physiol. Plant.	31	331-341
IT-Cas	Castellaro	Rossini et al.	2010	Agric. Forest Meteorol.	150	1283-1296
UA-Pet	Petrodolinskoye	Medinets et al.	2009	Ecology of the cities and recreation zones, ISBN 978-966-8885-28-0 (in russian)		103-107
UK-ESa	East Saltoun	http://www.geos.ed.ac.uk/abs/research/micromet/Current/esaltoun/				

Table A2. Summary of input data used in model base runs and tested for sensitivity in alternative runs.

Model runs	**LAI**	$\boldsymbol{h_c}$	**Temperature**	**Relative humidity**	**Stability corrections**
Base Runs					
ModLAI / MeasHc	Model default	Measured	Ambient	Ambient	Yes
Alternative Runs					
ModLAI / ModHc	Model default	Model default	Ambient	Ambient	Yes
MeasLAI / MeasHc	Measured	Measured	Ambient	Ambient	Yes
Surface Potentials	Model default	Measured	z_0’	z_0’	Yes
No stability correction (CBED)	Model default	Measured	Ambient	Ambient	No

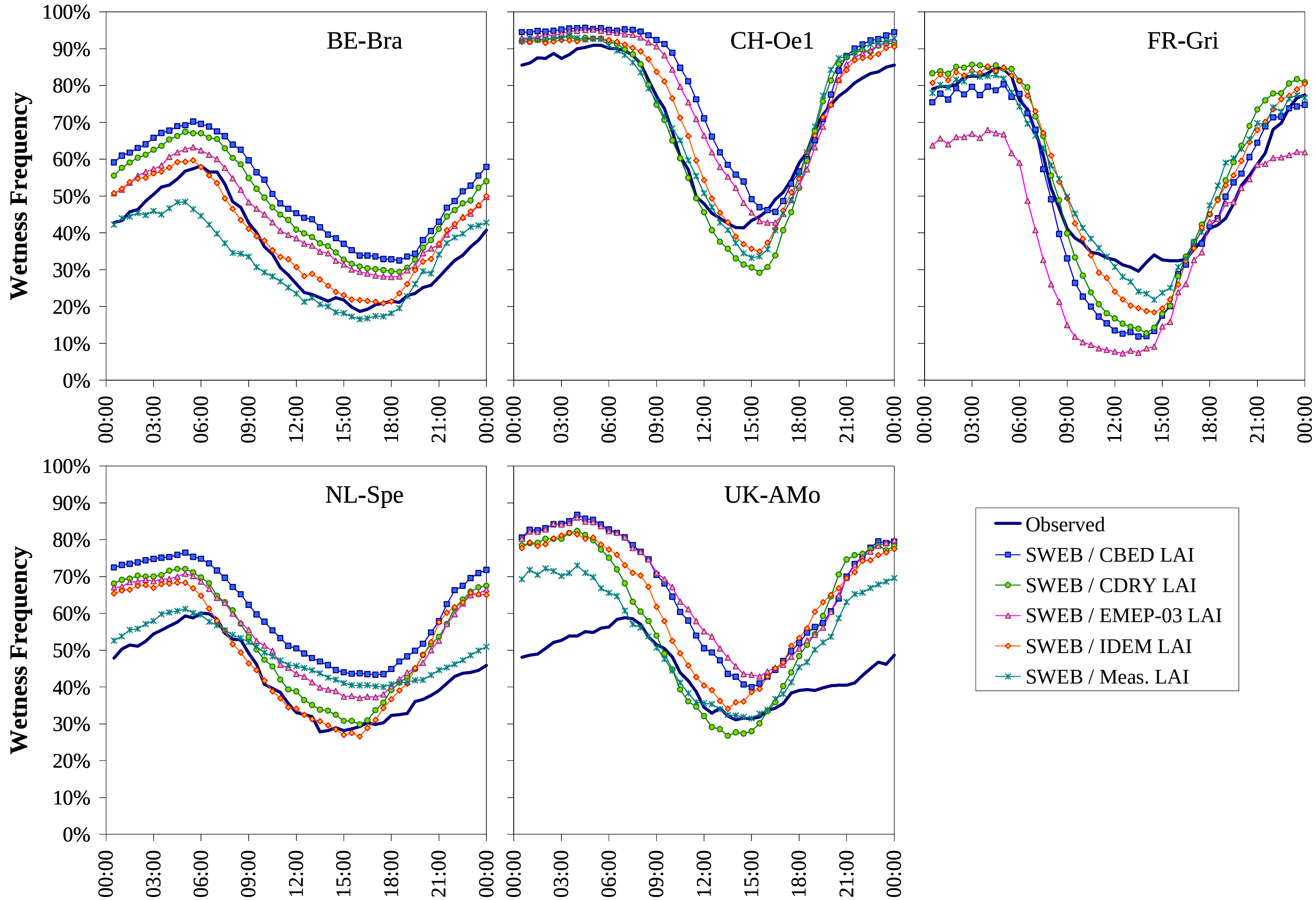

Figure A1. Comparison of observed and modelled annual diurnal cycles of canopy wetness frequency at five sites of the inferential network. Modelled values were obtained by running the surface wetness energy balance model (SWEB, Magarey *et al.*, 2006), using as input either the model default LAI values for each of CBED, CDRY, EMEP-03 and IDEM, or using the measured LAI.

Figure A2. Sensitivity of modelled annual N_r dry deposition fluxes to the choice of input data for LAI, h_c (measured vs model default), to the use of temperature and relative humidity at the surface (d+z_0') rather than ambient, and to the non-implementation of stability corrections (CBED only). The percentage differences are expressed relative to the model base runs as detailed in Table A2, with a negative number indicating larger dry deposition (or smaller emission), and a positive number indicating smaller dry deposition (larger emission).